



Universiteit
Leiden
The Netherlands

Doublecortin-like expressing astrocytes of the suprachiasmatic nucleus are implicated in the biosynthesis of vasopressin and influences circadian rhythms

Coomans, C.; Saaltink, D.J.; Deboer, T.; Tersteeg, M.; Lanooij, S.; Schneider, A.F.; ... ; Vreugdenhil, E.

Citation


Coomans, C., Saaltink, D. J., Deboer, T., Tersteeg, M., Lanooij, S., Schneider, A. F., ... Vreugdenhil, E. (2021). Doublecortin-like expressing astrocytes of the suprachiasmatic nucleus are implicated in the biosynthesis of vasopressin and influences circadian rhythms. *Glia*, 69(11), 2752-2766. doi:10.1002/glia.24069

Version: Publisher's Version
License: [Creative Commons CC BY-NC 4.0 license](https://creativecommons.org/licenses/by-nc/4.0/)
Downloaded from: <https://hdl.handle.net/1887/3209331>

Note: To cite this publication please use the final published version (if applicable).

RESEARCH ARTICLE

Doublecortin-like expressing astrocytes of the suprachiasmatic nucleus are implicated in the biosynthesis of vasopressin and influences circadian rhythms

Claudia Coomans | Dirk-Jan Saaltink | Tom Deboer | Mayke Tersteeg |
Suzanne Lanooij | Anne Fleur Schneider | Aat Mulder | Jan van Minnen |
Carolina Jost | Abraham J. Koster | Erno Vreugdenhil 

Department of Cell and Chemical Biology,
Leiden University Medical Center, Leiden, The
Netherlands

Correspondence

Erno Vreugdenhil, Department of Cell and
Chemical Biology, Leiden University Medical
Center, Leiden, The Netherlands.

Email: ernovreugdenhil@lumc.nl

Funding information

Diabetes Fonds

Abstract

We have recently identified a novel plasticity protein, doublecortin-like (DCL), that is specifically expressed in the shell of the mouse suprachiasmatic nucleus (SCN). DCL is implicated in neuroplastic events, such as neurogenesis, that require structural rearrangements of the microtubule cytoskeleton, enabling dynamic movements of cell bodies and dendrites. We have inspected DCL expression in the SCN by confocal microscopy and found that DCL is expressed in GABA transporter-3 (GAT3)-positive astrocytes that envelope arginine vasopressin (AVP)-expressing cells. To investigate the role of these DCL-positive astrocytes in circadian rhythmicity, we have used transgenic mice expressing doxycycline-induced short-hairpin (sh) RNA's targeting DCL mRNA (DCL knockdown mice). Compared with littermate wild type (WT) controls, DCL-knockdown mice exhibit significant shorter circadian rest-activity periods in constant darkness and adjusted significantly faster to a jet-lag protocol. As DCL-positive astrocytes are closely associated with AVP-positive cells, we analyzed AVP expression in DCL-knockdown mice and in their WT littermates by 3D reconstructions and transmission electron microscopy (TEM). We found significantly higher numbers of AVP-positive cells with increased volume and more intensity in DCL-knockdown mice. We found alterations in the numbers of dense core vesicle-containing neurons at ZT8 and ZT20 suggesting that the peak and trough of neuropeptide biosynthesis is dampened in DCL-knockdown mice compared to WT littermates. Together, our data suggest an important role for the astrocytic plasticity in the regulation of circadian rhythms and point to the existence of a specific DCL⁺ astrocyte-AVP⁺ neuronal network located in the dorsal SCN implicated in AVP biosynthesis.

KEYWORDS

astrocytes, circadian, doublecortin, plasticity, suprachiasmatic nucleus, vasopressin

This is an open access article under the terms of the Creative Commons Attribution-NonCommercial License, which permits use, distribution and reproduction in any medium, provided the original work is properly cited and is not used for commercial purposes.

© 2021 The Authors. *GLIA* published by Wiley Periodicals LLC.

1 | INTRODUCTION

The suprachiasmatic nucleus (SCN) constitutes the coordinator of daily rhythms in the body, such as circadian cortisol release and sleep–wake cycles (Abrahamson & Moore, 2001). This circadian rhythm is generated by the circadian molecular clock, which is comprised of two autoregulatory loops of clock genes, that take approximately 24 h to complete (Hastings et al., 2018). All individual neurons in the SCN have their own molecular clock and thus rhythm, but also work together thereby generating highly robust and coherent oscillations (Meijer et al., 2012).

The SCN is a heterogeneous structure which can be anatomically and functionally subdivided in a ventrolateral Vasoactive Intestinal Peptide (VIP) -expressing “core” region and a dorsomedial Arginine VasoPressin (AVP) -expressing “shell” region. The core region is sensitive to light information from the eye; the most important Zeitgeber that synchronizes the SCN (Morin, 2013). In contrast to the core, the shell exhibits a strong intrinsic, light-independent circadian rhythm (Lee et al., 2003). Also, the neurons in the shell of the SCN display a distinct phenotype compared to the core, as they do not express mature neuronal marker NeuN (Saaltink et al., 2012). In contrast to AVP in other brain nuclei, AVP is expressed in the SCN in a circadian manner (Li et al., 2009; Yoshikawa et al., 2015). The role of AVP in circadian timekeeping has been well established and is considered as the most important output signal from the SCN, as well as an internal neurotransmitter controlling the coupling of SCN neurons (Kalsbeek et al., 2010; Mieda et al., 2015).

The SCN has long been considered as a neuronal clock. However, recent studies clearly show that astrocytes in the SCN are equally important for the generation of circadian rhythms. Astrocytes express clock genes rhythmically and release their transmitters in a circadian fashion (Marpegan et al., 2011; Prolo et al., 2005). In rodents, astrocytes release glutamate rhythmically in the dark phase, which subsequently drives neuronal inhibition by activation of GABAergic neurons in the SCN. Moreover, genetic manipulations of clock genes specifically in astrocytes have demonstrated their pivotal role in the generation of circadian rhythms (Barca-Mayo et al., 2017; Brancaccio et al., 2017; Brancaccio et al., 2019; Tso et al., 2017). From these studies, the picture emerges that astrocytes orchestrate the activity of SCN neurons. Moreover, astrocytes in the SCN exhibit high levels of structural plasticity and change the shape of their projections in a day–night fashion (Bosler et al., 2015). These astrocytic structural rearrangements of the plasma membrane are mediated by endocytosis. However, the mechanism underlying this astrocytic structural plasticity and how this contributes to the generation of circadian rhythmicity is presently unknown.

Recently, we demonstrated the expression of a neuroplasticity protein, called Doublecortin-like (DCL), in the shell of the SCN (Saaltink et al., 2012). DCL is a microtubule-associated protein (MAP) that is implicated in neuroplasticity events in the developing and adult brain (Boekhoorn et al., 2008; Koizumi et al., 2006; Saaltink et al., 2012; Vreugdenhil et al., 2007). By means of phosphorylation and dephosphorylation events of its microtubule-binding domains

DCL regulates the stability of the cytoskeleton, thereby enabling structural rearrangements necessary for cellular migration (Schaar et al., 2004). In the embryonic brain, DCL is expressed in neuronal progenitor cells where it stabilizes mitotic spindles (Vreugdenhil et al., 2007). In the adult brain, DCL is expressed in a limited number of brain regions characterized by high levels of neuroplasticity (Saaltink et al., 2012). For example, DCL is expressed at the neurogenic niche of the dentate gyrus where it is important for neural progenitor cell migration and maturation (Saaltink et al., 2020). Besides its role in neurogenesis, DCL is involved in kinesin-dependent retrograde transport of signaling molecules (Fitzsimons et al., 2013; Lipka et al., 2016; Liu et al., 2012; Shin et al., 2013). Thereby, the C-terminal of DCL, which is located outside the microtubules (Moores et al., 2004), can interact with clathrin adaptor complex proteins AP-1 and AP-2 of the endocytic machinery, indicating a role for these proteins in endocytosis and vesicular trafficking (Friocourt et al., 2001).

The specific expression in the shell of the SCN and its biochemical and biophysical properties suggest an important role for DCL in the generation of circadian rhythms. Therefore, we have explored the functional significance of DCL by behavioral analysis of DCL knockdown mice and littermate controls, by immunohistochemistry and by electron microscopy. DCL knockdown mice exhibit significant shorter periods of their endogenous circadian cycle and adjusted faster to an 8-h shift in the light–dark cycle. In addition, we found that DCL is specifically expressed in astrocytes in the shell of the SCN that surround AVP-positive cells. As DCL-knockdown results in increased AVP cell volume and intensity and altered numbers of putative AVP dense core vesicles, we suggest that DCL-positive astrocytes regulate the biosynthesis of AVP. Together, our data point to the existence of a DCL-positive astrocytic network in the shell of the SCN that controls circadian rhythmicity by directing AVP biosynthesis.

2 | MATERIAL AND METHODS

2.1 | Animals

A transgenic DCL-knockdown mouse model of C57Bl/6J male mice (Charles River) has recently been described (Saaltink et al., 2020). This transgenic mouse contains an inducible sh-RNA, called DCL-KD mice, of which transcription can be induced by doxycycline (dox) via food pellets (Dox Diet Sterile S3888, 600 mg/kg, BioServ, New Jersey, USA; for technical background see Saaltink et al., 2020; Seibler et al., 2007). For all experiments, heterozygous sh-RNA and their littermate WT mice were used. Mice were put for 4 weeks on dox diet (Dox Diet Sterile S3888, 200 mg/kg, BioServ, NJ, USA) and fed ad libitum before they were used for any experiment. Mice tissues were obtained from DCL knockdown mice and wildtype littermates as controls. All animals were killed at ZT8 and/or ZT20 by decapitation and further processed as described (Saaltink et al., 2012).

All experiments were approved by the committee of Animal Health and Care, Leiden University and performed in compliance with

the European Union recommendations for the care and use of laboratory animals.

2.2 | Circadian behavior

Three-months-old male mice were individually housed with water and food available ad libitum. DCL knockdown mice or wildtype littermates were on a Chow diet or on a Dox diet, resulting in four experimental groups ($n = 8$ – 10 per group). At the beginning of the experiment, mice were exposed to a 12 h light/12 h dark regime and their locomotor activity was recorded by a Passive InfraRed sensor (PIR). The recorded locomotor activity was analyzed using Clocklab (Actimetrics). Under constant darkness (DD, 20 days), the free-running period (τ) and strength of the rhythm, was calculated for each mouse by means of a F-periodogram analysis. In this method a standardized root mean square amplitude is estimated as a function of the period, and a 99% confidence limit is determined based on the F-distribution. This method to determine the significant circadian period is applied to the 10-day intervals of each individual animal. The result is a line which peaks above the confidence limit when the period is considered to be significant. The strength of the circadian component is defined as the difference between the peak and the 99% confidence limit (Jenni et al., 2006; Panagiotou & Deboer, 2020; Stenvers et al., 2016).

To examine the role of DCL in the adaptation to a shifted light dark cycle we exposed the animals to a phase advance of 8-h and a phase delay of 8-h. The speed of adaptation to the new phase of the light-dark cycle was analyzed by determining onset of activity (advance) or offset of activity (delay) for each individual. Subsequently the day at which half the phase shift was completed (PS50, Kiessling et al., 2010) was determined for each animal individually.

IBM SPSS Statistics 23 was used to analyze the data obtained from Clocklab. Two-way-ANOVA with a post-hoc Tukey test was performed to determine differences between the four groups (WT + Chow, WT + Dox, DCL-KD + Chow, and DCL-KD + Dox) at the different time points. Differences in parameters of a group between different time points were determined by multiple paired *t*-testing.

2.3 | Immunohistochemistry

Three-months-old male mice DCL-KD mice ($N = 8$) and their littermates were anesthetized at ZT8 with Euthanasol and perfused with cold NaCl 0.9% (Braun, Melsungen, Germany) followed by perfusion with 4% para-formaldehyde (PFA) in 0.1 M PBS. The brain was then isolated and fixed in 4% PFA at 4°C for 24 h, and subsequently dehydrated in 15% sucrose at 4°C. Following dehydration, brains were saturated in 30% sucrose at 4°C before cryosectioning.

Serial coronal sections were obtained using a cryostat (Leica CM 1900, Leica Microsystems, Rijswijk, The Netherlands). Slicing was started at +3 Bregma up until –3 Bregma. The slices were stored in an antifreeze solution (40% 0.1 M TBS, 30% ethylene glycol and 30% glycerol) and stored at –20°C until further use.

Double-immunohistochemistry with fluorescence detection was performed as described previously (Saaltink et al., 2012). Briefly, sections were left at room temperature for 10 min before washing them three times with 0.1% Triton X-100 (Boom BV, Meppel, The Netherlands) in PBS. Following washing, the tissue was incubated with 0.3% Triton-X in TNB 0.1 M Tris-HCl pH 7.5, 0.15 M NaCl +0.5% Blocking reagent (Boehringer, Alkmaar, The Netherlands) for 1 h at room temperature. Primary antibodies were diluted in 0.3% Triton-X in TNB and incubated for 1 h at room temperature, following an overnight incubation at 4°C under gentle rotation for 24 h. Subsequently, sections were washed with 0.1% Triton X-100 in PBS incubated with secondary antibodies for 2 h and washed again with PBS. Free floating sections were dragged on a microscope glass and air dried for 4 h. Subsequently, 5 μ l of ProLong GOLD containing DAPI (ThermoFisher Scientific) was dropped on each section and the slides were covered with a coverslip. Experiments involving quantification or comparisons were conducted simultaneously. Immunofluorescence was detected by the Leica DM5500 and/or Leica SP8 confocal microscope and analyzed using Las X software. Primary antibodies were derived from Temecula California (AVP, AB1565, (Jimenez et al., 2015; Sonnevile et al., 2010) or Bachem, Bubendorf, Switzerland (anti-AVP; T-5048) for AVP-DCL doublelabeling experiments, Abcam (GFAP, AB4674), SantaCruz (S100b C-20, SC7851) and Synaptic Systems (GAT3, 274,304). The DCL antibody was homemade and has been described in detail (Saaltink et al., 2012). Secondary Alexa fluor antibodies were derived from ThermoFisher (A31573, A32731, A21432) and Life Technologies (A11039). The percentage of AVP⁺/DCL⁺ cells was determined by counting the total number of AVP⁺ cells and the number of AVP⁺ cells that were not engulfed by DCL⁺ rings in the SCN of 4 mice (2–3 slices/per mouse). The number, volume and signal intensity of AVP cells and varicosities in the shell and in the core of the SCN were inspected by analyzing Z-stacks (3 SCN-containing sections per animal) using by Image Pro Premier 3D (IPP 3D) version 9.3 (Media Cybernetics). Data obtained by IPP 3D analysis was statistically analyzed using Graphpad Prism 7.0 and using unpaired *t*-tests.

2.4 | Electron microscopy

The effect of DCL knockdown on AVP expression in neurons of the SCN was investigated with transmission electron microscopy (TEM). DCL knockdown mice and wild-type littermates on dox diet were sacrificed on time points ZT 8 and ZT 20. Two hundred micrometer thick vibratome sections of the posterior part of the suprachiasmatic nucleus (SCN) bordered by the third ventricle and the optic chiasma were made. Sections were immersed in 1,5% glutaraldehyde (GA)/0,1 M cacodylate buffer. After a 2-h fixation at room temperature, sections were rinsed with 0,1 M cacodylate buffer three times followed by a 1 h postfixation in 1%OsO₄/0,1 M cacodylate buffer on ice. After rinsing with 0,1 M cacodylate, sections were dehydrated with an ascending series of ethanol, followed by propylene oxide and EPON (LX112) mixtures, and EPON alone. Vibratome sections were subsequently flattened, orientated and embedded in embedding

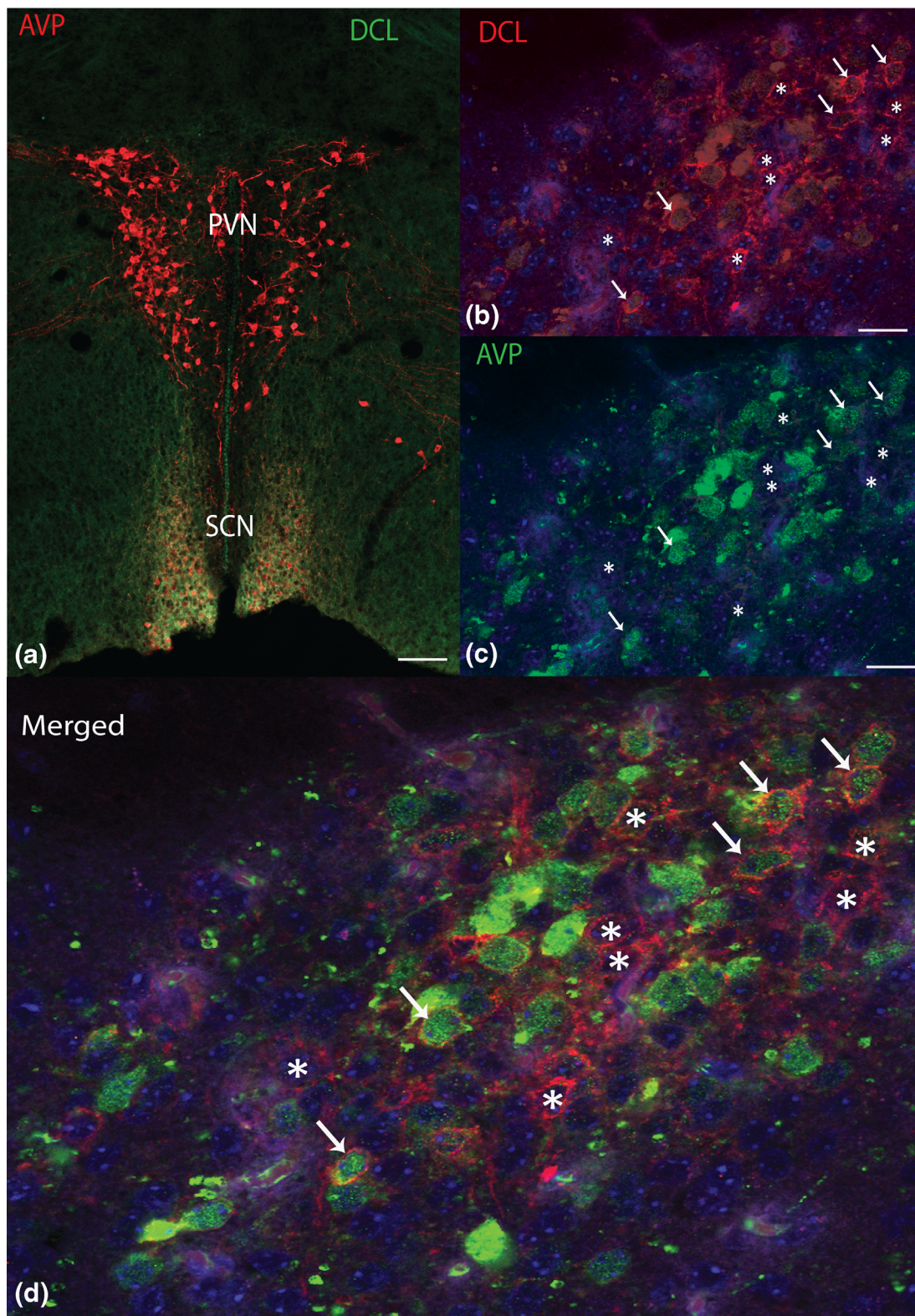


FIGURE 1 Confocal microscope analysis of DCL and AVP expression in the SCN. (a) Low power picture showed specific expression of AVP (red) in the paraventricular nucleus (PVN), while DCL (green) is colocalised with AVP in the SCN. Scalebar: 100 μ m. (b–d) Higher magnification of DCL (red, B and D) immunoreactivity is present in ring-like structures that seems to engulf AVP-positive neurons (green, c and d). Arrows indicate overlap of DCL and AVP expression. Asterisks highlight DCL-positive rings surrounding AVP-negative cells. Animals (N = 8; 3 sections per animal) were sacrificed at ZT8. Blue color: DAPI. Scalebar: 20 μ m

molds. After polymerization of the EPON for 2 days at 60°C degrees sections of 80 nm thickness were made and collected on one-hole grids. After staining with uranyl acetate and lead citrate the sections were examined with TEM at 120 kV (FEI Tecnai T12twin, camera: oneview, Gatan). Overlapping images were collected and stitched together into separate images as previously described (Faas et al., 2012). The area imaged always contained the SCN area and part of the bordering third ventricle and /or the optic chiasma allowing the precise localization of the SCN.

Stitches were scored by two independent persons without knowledge of the background, and with a magnification of 11,000x and image resolution of 2 micron. Dense core vesicles were defined as having a round shape with a diameter between 85–120 nm, and containing a dark core with a halogenic boundary (Castel et al., 1990). The amount of DCV-containing neurons were counted, which were defined as neurons containing a minimum of 5 dense core vesicles. Cells were considered neurons when they possessed a clear cell boundary and a round, nonlobed nucleus. Non-neuronal cells were considered to contain cytoplasm that is hard to distinguish from the extracellular matrix, and a nucleus with a lobed structure. All cells visible in the stitches were counted, with the exception of cells that were not fully on the stitch.

3 | RESULTS

3.1 | DCL expression in GAT3-positive/GFAP-negative astrocytes and GAT3-positive varicosities of the SCN

We have previously shown DCL expression in the shell of the SCN where it colocalizes with AVP (Saaltink et al., 2012). However, the cellular origin of DCL expression in the shell is unknown. To investigate the cellular origin in more detail, we analyzed DCL and AVP immunoreactivity with confocal microscopy at high resolution. In line with our previous results, we observed specific AVP expression in the PVN, while DCL is colocalised with AVP in the SCN (Figure 1a). Remarkably, we observed DCL immunoreactivity in ring-like structures (Figure 1b,d) that seems to envelop cells in the shell region of the SCN. AVP immunoreactivity was found mainly in cell bodies, which is in line with previous reported studies (Figure 1c,d; Lee et al., 2003). Dual labeling pictures indicated that 87% (± 0.034) of AVP-positive cells were enveloped by DCL-positive cells. However, little, if any, DCL immunoreactivity colocalized with AVP, suggesting that DCL is expressed in other cell types than AVP-positive neurons. To further characterize DCL-positive cells in the SCN, we have performed series of double immunohistochemical labeling experiments with anti-DCL and cell-specific markers. S100- β is a marker for cortical astrocytes. However, we found no Immunohistochemical staining with anti-S100- β antibodies in the SCN, while we found clear S100- β -positive cells in the cortex (data not shown), suggesting that S100- β -positive astrocytes are not present in the SCN. Immunohistochemical staining with the general astrocyte marker glial fibrillary acidic protein

(GFAP) gave clear signals in fiber-like structures in the core of the SCN but little GFAP immunoreactivity was observed in the shell of the SCN (Figure 2a,d). In line with this, colocalization of GFAP and DCL immunoreactivity did not occur (Figure 2c,f), indicating that DCL-positive cells in the SCN are GFAP-negative. The pattern of

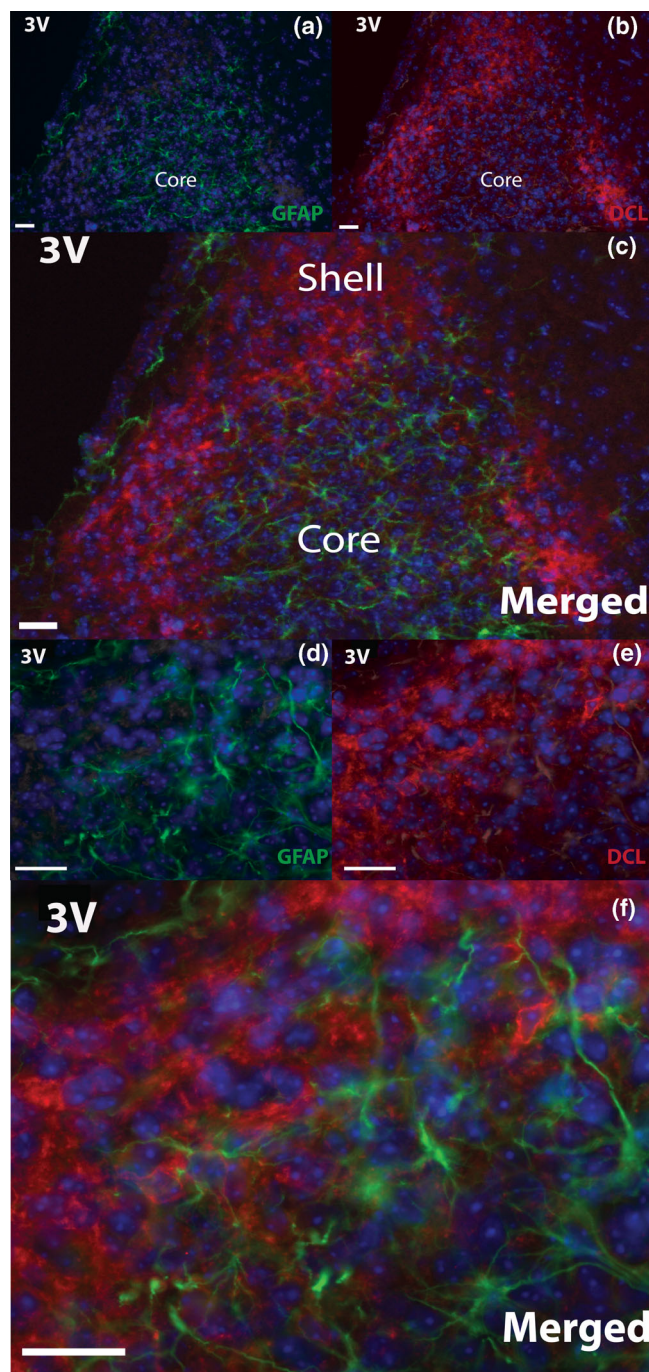


FIGURE 2 Confocal microscope analysis of DCL and GFAP expression in the SCN. DCL (red, b, c, e, and f) immunoreactivity is present mainly in the shell of the SCN. GFAP (green, a, c, d, and f) immunoreactivity is mainly present in the core of the SCN in fiber-like structure. Note the lack of colocalization of DCL and GFAP. Animals ($N = 8$; 3 sections per animal) were sacrificed at ZT8. Blue color: DAPI. Scale bar: 20 μ m

DCL-positive immunoreactivity is reminiscent of the astrocyte specific GABA transporter GAT3 that has been reported to surround AVP and VIP-positive neurons in the SCN (Moldavan et al., 2015). Therefore, we stained the SCN with GAT3-recognizing antibodies and -as reported (Moldavan et al., 2015)-found abundant immunoreactive

signals in both the core and shell of the SCN (Figure 3a,b). Similar as with DCL immunohistochemical staining patterns, GAT3 immunoreactivity is present in ring-like structures that partially overlap with DCL (Figure 3c,d). Noticeably, both GAT3 and DCL display a speckled staining pattern (see also Figure 1).

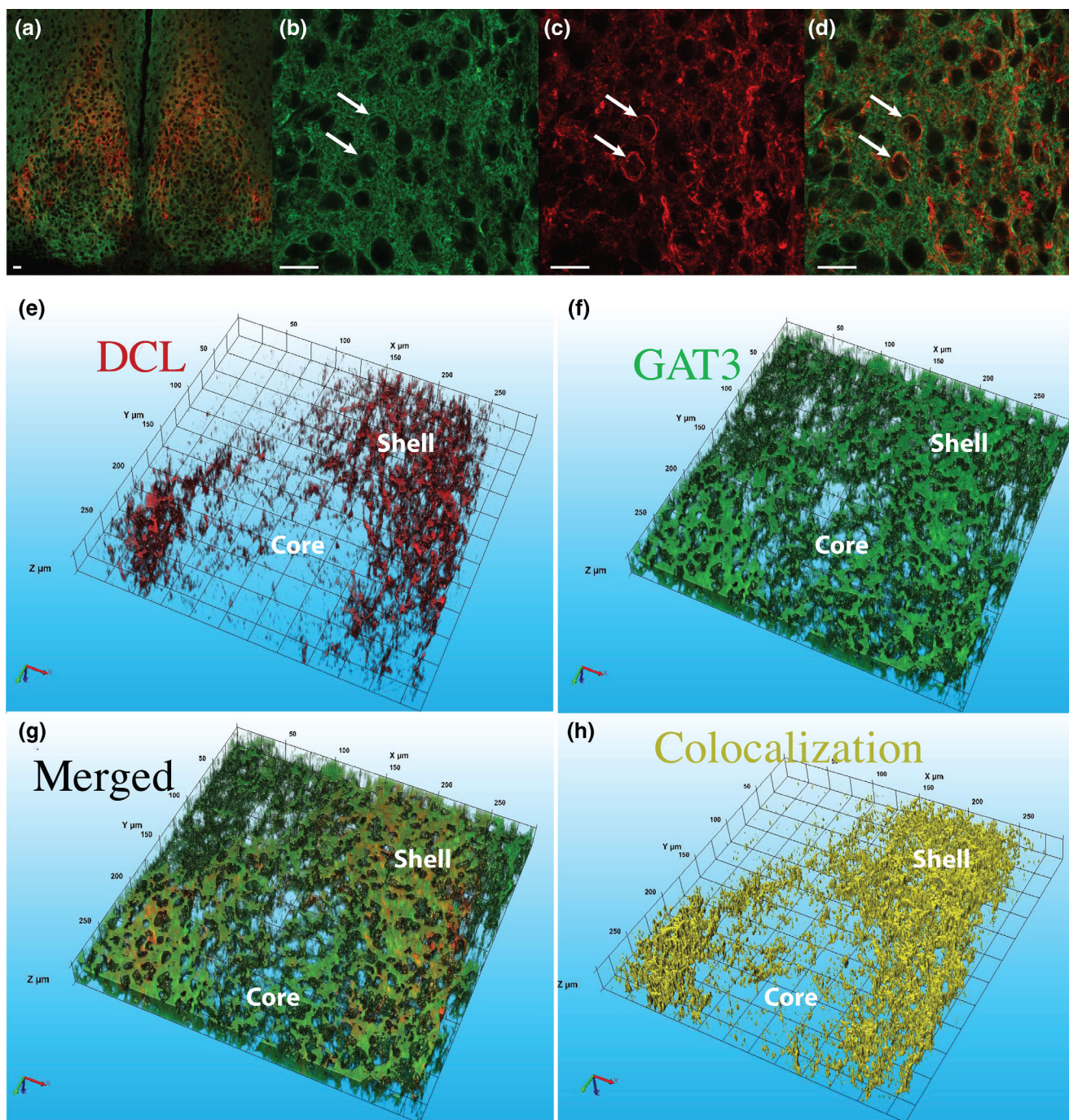


FIGURE 3 Colocalization of DCL with the astrocyte marker GAT3 in the SCN. (a) Overview of GAT3 and DCL in the SCN. (b) as reported (Moldavan et al., 2015), GAT3 immunoreactivity is present in ring-like structures in the SCN. (c) DCL immunoreactivity is also present in ring-like structures (arrows; see also Figure 1) (d) merged picture showing DCL (red) and GAT3 (green) immunoreactivity in the SCN. Scale bar (a–d): 10 μm. (c–e) 3D reconstructions of DCL (red) and GAT3 (green) expression in the SCN. DCL (e and g) is mainly present in the shell with numerous DCL-positive varicosities in the core. GAT3 immunoreactivity (f and g), is broadly present throughout the SCN. Note that DCL-positive immunoreactivity colocalizes (h: Yellow) with that of GAT3, not only in the shell but also in the varicosities in the core of the SCN. Animals (N = 8; 3 sections per animal) were sacrificed at ZT8



To further investigate possible colocalization of GAT3 and DCL expression, we performed detailed 3D reconstructions from confocal Z-stacks for GAT3 and DCL immunoreactivity. We found the 70.3% of the DCL immunoreactivity colocalized with GAT3 immunoreactivity (see Figure 3). Remarkably, numerous DCL-positive varicosities in the core of the SCN (Figure 3a), where also positive for GAT3. Taken together, we conclude that DCL is expressed in GAT3-positive/GFAP-negative astrocytes and GAT3-positive varicosities in the SCN.

3.2 | DCL shortens the free running period and the time to adjust after phase shifts of the light dark cycle

To explore whether or not possible DCL-mediated plasticity in the SCN is important for the generation of circadian rhythmicity, we have used heterozygous doxycycline-inducible DCL-KD mice and their WT littermates (Saaltink et al., 2020) and analyzed the free running period and phase shifting in these mice. In line with DCL knockdown efficacy after doxycycline administration in the hippocampus (Saaltink et al., 2020), we observed a 59.37 ($\pm 4.98\%$) knockdown in the SCN in DCL-KD mice, compared to WT littermates fed on doxycycline (See Figure 4). DCL-KD mice on chow displayed the same free running period and phase shifting capacity as WT littermates on chow or on dox-diet. We have investigated the free running period of DCL-KD mice during 10 consecutive days in constant darkness. Compared to WT littermate controls on a dox-diet, DCL-KD mice exhibit a significant ($p < .05$; $n = 8$) shorter period of 23.8 h (Figure 5a). Rhythm strength in both light-dark conditions and constant darkness, measured with F-periodogram analysis, was lower in DCL-KD mice (Figure 5d). Next, we housed mice on a 12 h light and 12 h dark (LD) cycle for 5 weeks and advanced the LD cycles by 8 h (Figure 5b,c,e,f). Wildtype animals re-entrained their rest-activity gradually to the new phase of the light-dark cycle by approximately 1 h/day (Figure 5e). However, the DCL-KD mice entrained approximately twice as fast as their littermate controls (PS50 respectively 3.5 days versus 6.25 days; $p < .001$). Similarly, also a phase delay of

8 h resulted in significant faster re-entrainment of DCL-knockdown animals (PS50 respectively 2.5 days versus 3.75 days; $p < .001$). Therefore, we concluded that DCL expression is implicated in the robustness of the circadian rhythm and its entrainment to the external light-dark cycle.

3.3 | The biosynthesis of neuropeptide transmitters in the SCN is affected by DCL knockdown

The enveloping of AVP+ cells by DCL expressing projections in the shell of the SCN suggest a possible interplay between DCL-positive astrocytes and AVP signaling. Moreover, similar as in our DCL-KD mice, previous studies have revealed that a lack of AVP signaling resulted in faster entrainment to a shifted light-dark cycle (Yamaguchi et al., 2013). Therefore, we investigated the effect of DCL knockdown on AVP signaling in the SCN by means of immunohistochemistry and TEM.

Compared to WT littermates (Figure 6a), staining with AVP antibodies revealed more intense immunoreactivity with more AVP-positive cells in the shell of the SCN of DCL-KD mice, both on dox diet (Figure 6b). To investigate this in more detail, we analyzed confocal Z-stacks and made 3D reconstructions of the SCN in order to calculate the number, volume and total luminescence of AVP-positive cells in DCL knockdown and wildtype littermates (Figure 6c-i). Compared to WT littermates, DCL-KD mice had significant more AVP-positive cells (Figure 6g, respectively 33.67 ± 6.14 versus 67.31 ± 10.21 ; $p = .005$; $N = 8-9$). Also, the fluorescence intensity was also significantly higher in DCL-KD animals (Figure 6h, $312,705 \text{ lum} \pm 104,179$ versus $21,815 \text{ lum} \pm 16,084$; $p = 0.049$), and the average volume of AVP-positive cells was significantly larger in DCL-KD mice (Figure 6i, $150.9 \mu\text{m}^3 \pm 4.67$ versus $131.9 \mu\text{m}^3 \pm 4.97$; $p = .007$). Of note, the variation within groups of the experimental data seemed higher in the DCL-KD group than in the WT group. We conclude that DCL may affect the AVP protein levels in the SCN.

The shell of the SCN is known to express an numerous neuropeptides such as Neuromedin-S, Prokineticin-2, met-Enkephalin and AVP

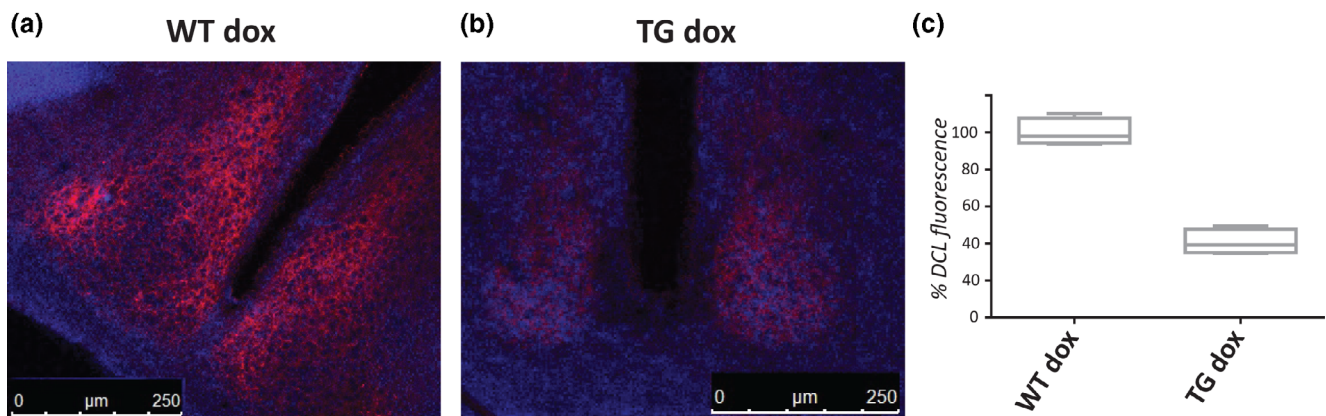


FIGURE 4 Knockdown efficacy of DCL in WT and TG mice after 4 weeks of doxycycline (dox) administration in food pellets. Representative confocal picture with the SCN of a WT (a) and TG (b) are shown. Knockdown efficacy is 60% as deduced from DCL fluorescence. Animals ($N = 8$; 3 sections per animal) were sacrificed at ZT8

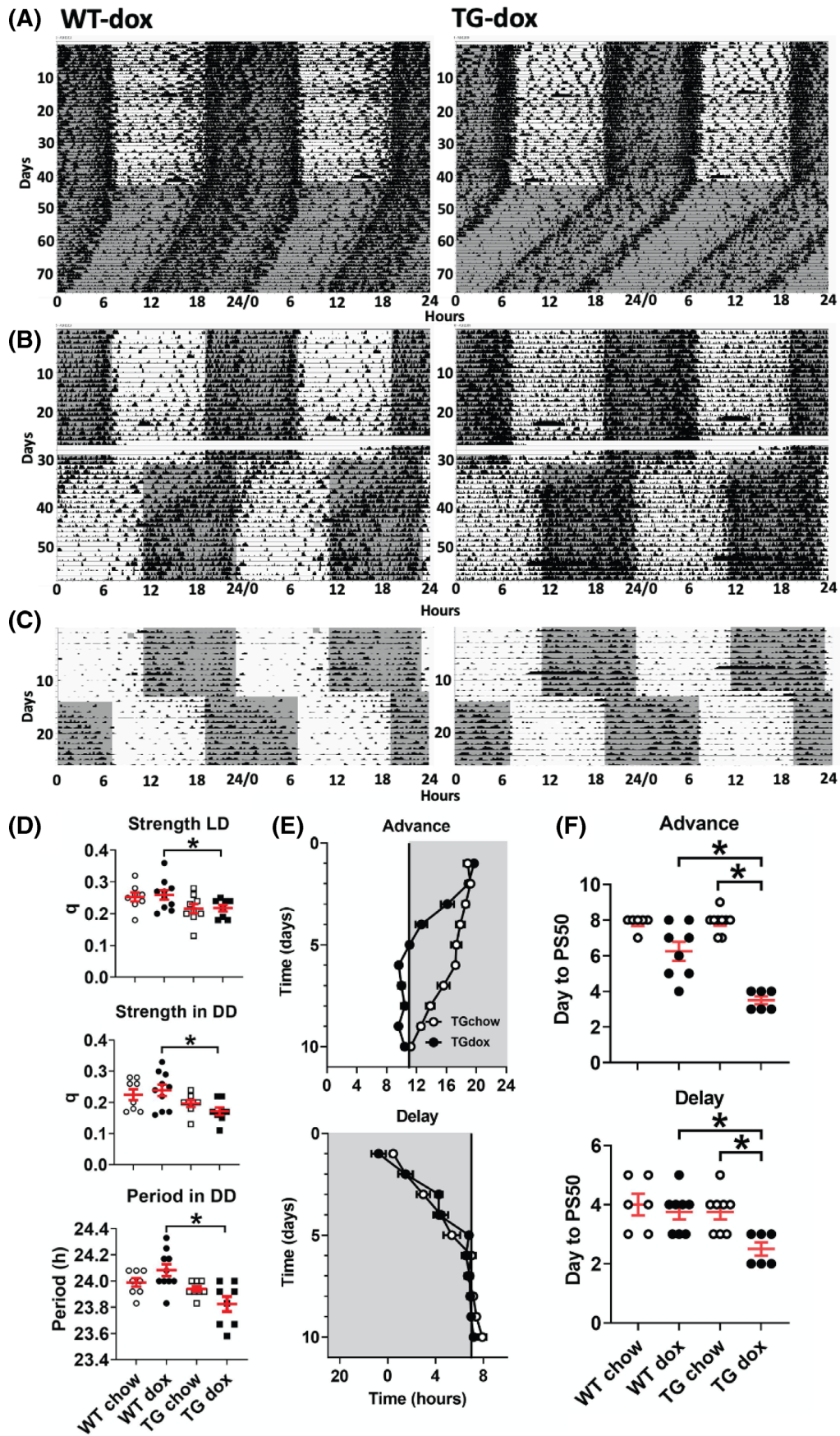


FIGURE 5 Legend on next page.



(Abrahamson & Moore, 2001; Park et al., 2016; Wen et al., 2020). To investigate the effect of DCL knockdown on the biosynthesis of such neuropeptides in the SCN and their possible circadian expression at the subcellular level, we inspected SCN brain slices of DCL-KD mice and WT mice with TEM. We analyzed our TEM preparations in a morphometric manner by counting the total number of neurons. We defined neurons as cells having a round nucleus with clear cytoplasm and bearing dense core vesicles (DCV), showing an electron lucent halo and with a diameter of between 85–120 nm that putatively contain neuropeptides (Figure 7a–d, Castel et al., 1990). In addition, we determined the outline of the nucleus and cytoplasm of the putative neuropeptide-positive neurons as defined above. In line with a circadian rhythm for neuropeptide biosynthesis, we observed a significant difference in the percentage of DCV-containing neurons between the wildtype mice sacrificed at ZT8 (49.1%) and ZT20 (19.2%, $p < .001$; Figure 7e). In contrast, the percentage of DCV-containing neurons in DCL-KD was 38.9% at ZT8 and 33.1% at ZT20, which was significantly different compared to WT littermates (respectively $p = .029$ and $p = .013$). We also observed a significant difference ($p = .014$) in mean cell: nucleus ratio at ZT8, which is higher in the DCL-KD group (1.73 ± 0.13) compared to the wildtype group (1.54 ± 0.12). At ZT20 however, we found no difference in the cell: nucleus ratio between the two genotypes (Figure 6e). We conclude from these EM studies that DCL knockdown may dampen the circadian rhythmicity of neuropeptide biosynthesis in the SCN.

4 | DISCUSSION

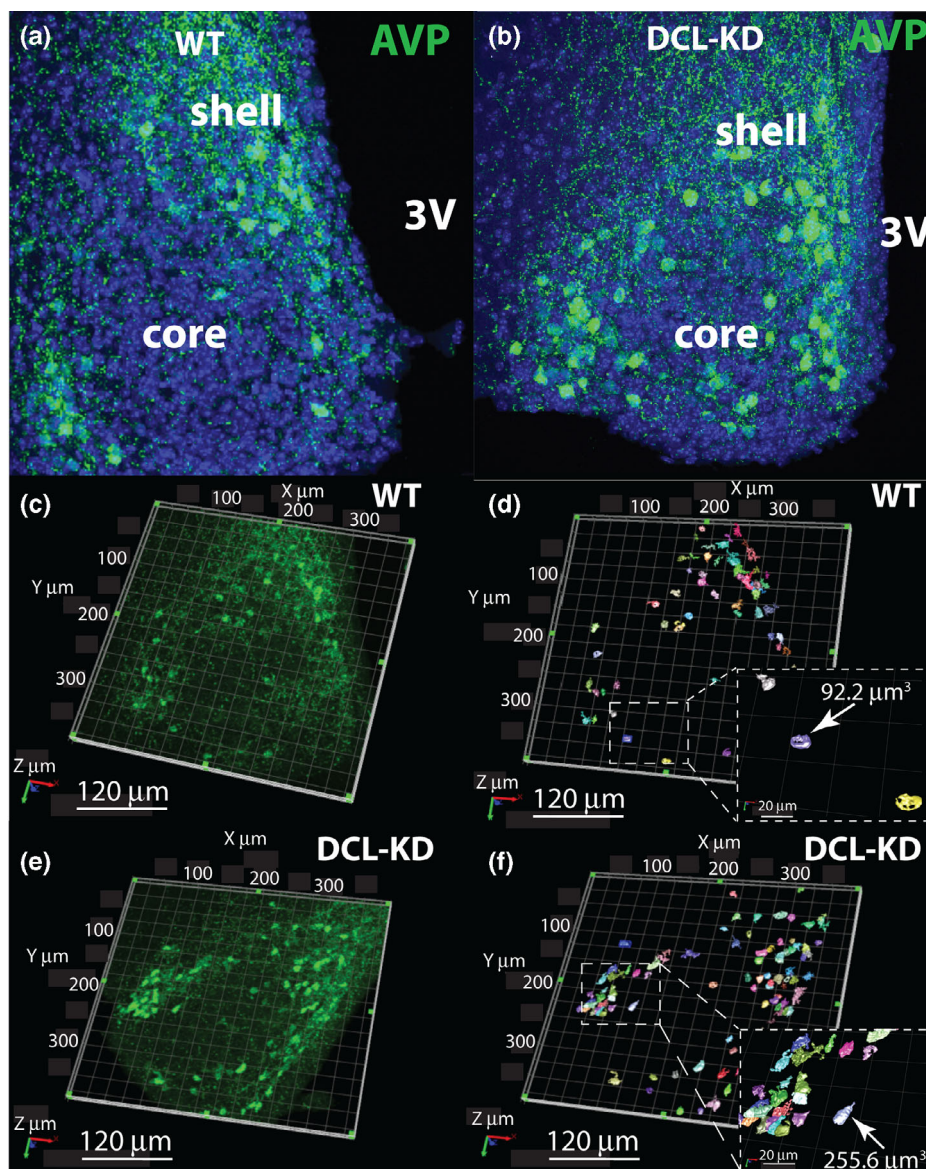
We investigated the functional significance of DCL, a neuroplasticity protein, that is expressed in an overlapping fashion with AVP in the shell of the SCN by means of immunohistochemistry and by analysis of circadian-related behaviors. We found that DCL is expressed in a subpopulation of astrocytes that enveloped AVP-positive cells and which are negative for the general glia marker GFAP but positive for the GABA transporter GAT3. Knockdown of DCL shortens the free running period and these mice re-entrain to novel time period almost twice as fast as their WT control. Surprisingly, knockdown of astrocytic DCL affects the biosynthesis of AVP by dampening the circadian fluctuation of AVP levels. Together, our data indicate that plasticity in a subgroup of astrocytes may regulate circadian behavior and the biosynthesis of neuronal AVP, thereby further highlighting the emerging importance of astrocytes in time keeping.

DCL is expressed in GAT3-positive/GFAP-negative astrocytes in the shell of the SCN. The finding that DCL-positive cells are GFAP-negative is remarkable as GFAP is generally considered as a glia marker. However, GFAP-negative glia cells represent a large portion (40%) of all glia (Walz & Lang, 1998) and GFAP-positive astrocytes have been found mainly in the ventrolateral region of the SCN (Becquet et al., 2008; Deng et al., 2010), which is in line with our GFAP staining. Also, the speckled pattern of DCL-positive immunoreactivity is very similar to that of GAT3, colocalizing in both varicosities in the core and cells in the shell, thus suggesting a link between DCL and GAT3. A similar expression profile of GAT3 in the SCN has been previously described (Moldavan et al., 2015) showing the presence of GAT3 in astrocytic projections engulfing neuronal cells. Also, these GAT3-positive astrocytes are largely GFAP-negative. However, in line with our findings, GAT3 has been reported to be evenly expressed in both core and shell (Moldavan et al., 2015), while DCL is specifically expressed in the shell of the SCN. Thus, next to the heterogeneous neuronal population, our studies point to the existence of a heterogeneous population of astrocytes in the central biological clock.

Based on the physiological properties of DCL, our study suggests an important role for rapid structural plasticity of astrocytes in the shell of the SCN. Indeed, astrocytes display striking circadian morphological plasticity in the rat dorsal SCN with long processes enwrapping neurons in the light period and short processes in the dark period (Becquet et al., 2008; Girardet et al., 2013, for review see Bosler et al., 2015). However, circadian plasticity of such astrocytic processes was identified with GFAP and our data indicate that DCL-positive cells are GFAP-negative. DCL may mediate circadian plasticity of astrocytic projections in the dorsal SCN. In line with such a function is the SP-rich C-terminal domain in DCL which is known to interact with $\mu 1$ and $\mu 2$ subunit of the AP1 and AP2 adaptor complex (Friocourt et al., 2003). AP2 is directly involved in clathrin-mediated endocytosis, a process necessary for plasma membrane internalization and thus necessary for the circadian plasticity of astrocytes. DCL also interacts with Usp9x (Friocourt et al., 2005), a deubiquitination enzyme. Moreover, crystallization studies demonstrated resemblance of DCL domains with ubiquitin (Kim et al., 2003), a protein well-known to be crucial not only for degradation via the proteasome but also for endocytic trafficking. Thus, DCL has several functional domains enabling interaction with the ubiquitin-endosomal system, which is necessary for rapid plasma membrane internalization. However, whether or not DCL is involved in all these processes in the SCN is presently unknown and requires further investigation.

FIGURE 5 DCL knockdown mice have shorter free running periods and show faster re-entrainment to a novel light–dark cycles. Representative double-plotted actograms of DCL knockdown mice on chow (left panels) and doxycycline (right panels) to investigate free running periods (a), an 8 hrs phase advance (b) of phase delay shift (c). The data in panel b and c are records from the same animals. Black bars indicate activity. Light gray and dark gray indicate lights-on and lights-off respectively. (d) a boxplot of the strength of the rhythm in LD (top), DD (middle) and free-running period in DD (bottom) of each group ($N \geq 8$) during the last 10 days of the DD period. The DCL-knockdown mice treated with doxycycline have a significantly weaker rhythm and significantly shorter free-running period, compared to littermate controls ($*p < .05$ t-test after significant 2-way ANOVA factor “genotype” * “diet”). E) Mean and SE of onset (top) and offset (bottom) of activity during an 8 h advance (top) or delay (bottom) of the light dark cycle. F) PS50 in the phase advance (top) and phase delay (bottom). $*p < .05$ t-test after significant 2-way ANOVA factor “genotype” * “diet”

FIGURE 6 Immunohistochemistry of AVP in the SCN of DCL knockdown animals and WT littermates. (a) Representative confocal microscope picture of AVP (green) immunoreactivity in WT mice. (b) Confocal microscope analysis of AVP (green) immunoreactivity in DCL knockdown (DCL-KD) mice. Note that compared to wildtype, the number and intensity seems increased in DCL-knockdown animals. (c and d) confocal Z-stack (c) and corresponding 3D reconstructions (d) of AVP positive cells in WT mice. (e and f). Confocal Z-stack (e) and corresponding 3D reconstructions (f) of AVP positive cells in DCL-KD mice. The dashed rectangles in d and f show larger magnifications of individual 3D AVP-positive cells. The corresponding volume of these individual cells, respectively $92.2 \mu\text{m}^3$ in WT and $255.6 \mu\text{m}^3$ in DCL knockdown mice, is indicated in the rectangles. The difference in colors in D and F indicate differences in cell volume. (g–i) quantification of the mean number (g), mean intensity (h, in lum) and mean volume (i, in μm^3) of AVP-positive cells in the SCN in DCL knockdown animals ($N = 8$; 3 sections per animal) and littermate WT controls ($N = 8$ –9; 3 sections per animal; $*p < .05$, $**p < .01$; $N = 8$)



Our results suggest a role for DCL+ astrocytes in the SCN in circadian rhythmicity. However, DCL is expressed in a few other brain regions such as hypothalamic tanycytes, the rostral migratory stream, the olfactory bulb, the islands of Calleja and the subventricular zone of the hippocampus (Saaltink et al., 2012). Some of these brain regions, such as the olfactory bulb and hippocampus have afferent connections with the SCN (Krout et al., 2002). Therefore, we cannot exclude the possibility that DCL knockdown, as is the case in the hippocampus (Saaltink et al., 2020), is (partly) responsible for our

observations. However, given the central role of the SCN in the generation of circadian rhythms and the recently established crucial position of astrocytes in the dorsal SCN (Brancaccio et al., 2019), we favor the view that DCL+ astrocytes in the SCN are the main contributor of altered circadian rhythmicity in the DCL knockdown mice.

Our TEM results show a correlation between DCL+ astrocytes and circadian neuropeptide biosynthesis in the shell of SCN. Likely, the majority of DCV-containing cells represent AVP expressing neurons as AVP is the most abundant neuropeptide transmitter in the

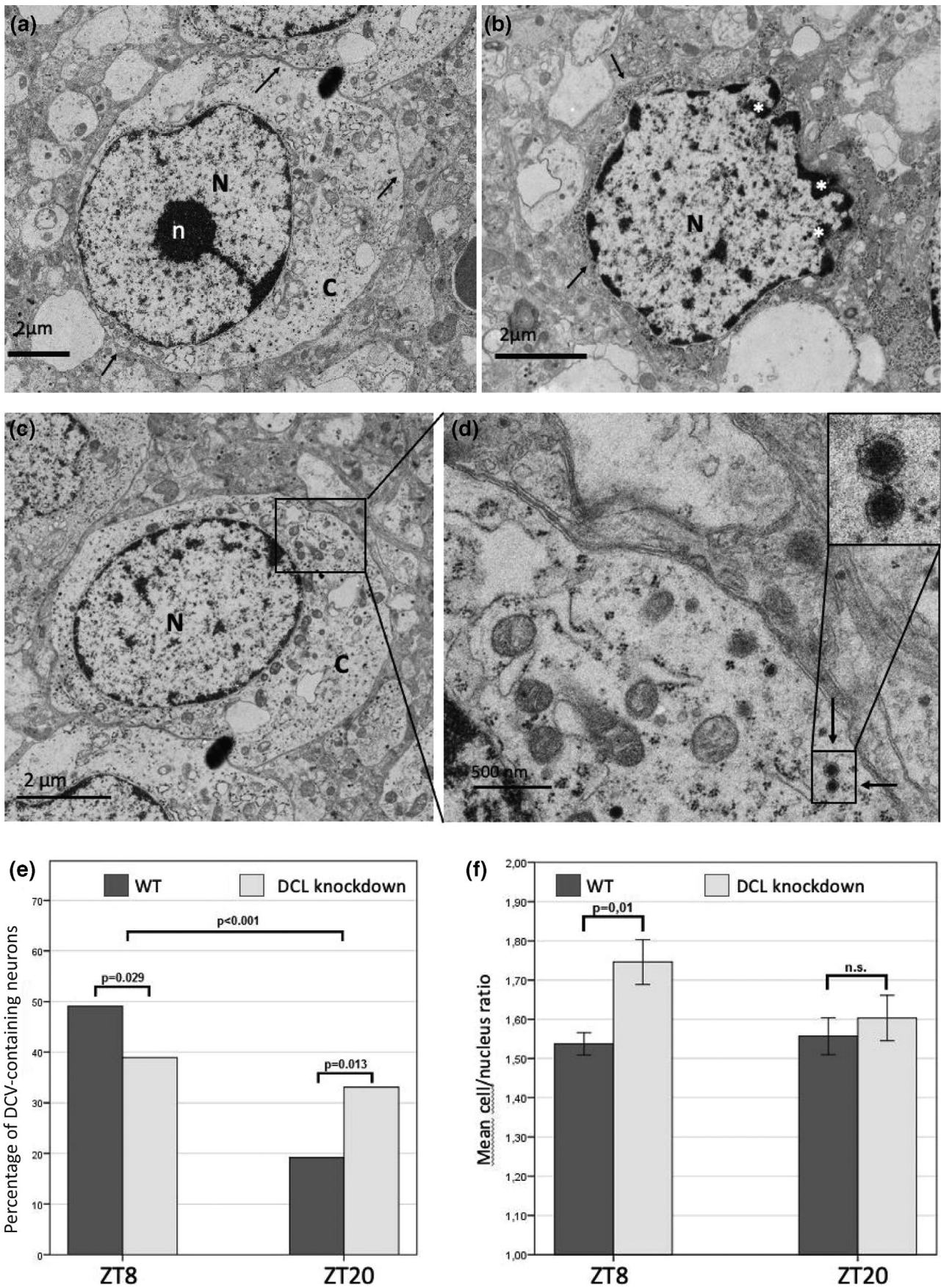


FIGURE 7 Legend on next page.

SCN (Abrahamson & Moore, 2001) and our observed circadian fluctuations with high levels at ZT8 and low levels at ZT20 correspond with reported circadian AVP expression (Dardente et al., 2004). In addition, the size of DCV's corresponds with those of AVP DCV's in the SCN (Castel et al., 1990). However, in addition to AVP, other neuropeptides, like Neuromedin-S, Prokinectin-2 and met-Enkephalin are expressed in the dorsal part of the SCN. (Abrahamson & Moore, 2001; Moore et al., 2002; Park et al., 2016; Wen et al., 2020). It is possible that these neuropeptidergic neurons are also interacting with DCL⁺ astrocytes. Indeed, the presence of numerous AVP-negative cells engulfed by DCL⁺ astrocytes (see Figure 1b–d), suggests such additional interactions. However, whether or not these interactions exist and their functional implications has to await careful double-labeling and behavioral studies in DCL-knockdown mice.

DCL knockdown leads to a shorter circadian period, reduced rhythm strength, and faster adjustment to a phase shift of the light–dark cycle, the latter approximately twice as fast as WT mice. Although the underlying mechanisms are unknown, we suggest a role for GABA and/or AVP signaling in these behavioral effects of DCL knockdown. We observe a large DCL-GAT3 colocalization, including in varicosities in the core of the SCN. Therefore, it is likely that the ability to take up GABA by GAT3 is altered by DCL-mediated plasticity of DCL/GAT3-positive astrocytes. Indeed, GABA has been shown to transmit phase information between the shell and core (Albus et al., 2005) and activation of GABA_A receptors during inhibited light-induced phase delays (Ehlen & Paul, 2009). Similarly, AVP-positive neurons are critical for coupling of neurons in the SCN (for review see [Mieda, 2019]) and deletions of AVP receptors dramatically shorten the time to adjust to novel time zones (Yamaguchi et al., 2013). However, in contrast to the effect of DCL knockdown, deletion of the AVP V1a receptor gene leads to a lengthening of the free running period in constant darkness (Li et al., 2009), suggesting that other signaling routes are affected by the DCL knockdown. Indeed, several neuropeptide transmitters other than AVP are expressed in the shell of the SCN (Moore et al., 2002) and several DCL-positive ring-like structures seem to surround AVP-negative neurons (see Figure 1).

Our findings that DCL-knockdown affect phase shifts, rhythm strength, and free running behavior further highlights the importance of astrocytes in circadian time keeping. In *Drosophila*, disruption of vesicle trafficking and elevation of calcium levels in astrocytes leads to loss of rhythmicity without affecting the cyclic expression of clock proteins (Ng et al., 2011). In mammals, astrocytes display circadian rhythms in ATP production that depends on mitochondrial calcium

production (Burkeen et al., 2011; Marpegan et al., 2011), and exhibit diurnal oscillations in glutamate uptake (Leone et al., 2015). Also, deletion of clock genes specifically in SCN astrocytes dampens the rhythmic expression of neuronal clock genes and regulates circadian behavior (Barca-Mayo et al., 2017; Tso et al., 2017). Recent exciting data revealed that activity of astrocytes is in antiphase with neuronal activity (Brancaccio et al., 2017). Astrocytes located in the dorsal region of the SCN, are active at night when they release glutamate, thereby suppressing the activity of SCN neurons likely via GABAergic signaling. During the day, extracellular glutamate decreases, enabling neuronal activity to occur. All these findings are in accordance with the reduced rhythm strength found in the DCL-knockdown group in the present study. Moreover, rhythmic astrocytes seems sufficient to create a functional SCN that drives circadian behavior (Brancaccio et al., 2019). These studies strongly indicate a pivotal role for astrocytes in the generation of circadian rhythms that seems equally important to that of neurons.

The change in biosynthesis of AVP in DCL knockdown mice suggest specific crosstalk between structural plasticity in astrocytes and the expression of AVP in the SCN. Precisely how DCL-positive astrocytes regulate AVP biosynthesis is at present unknown. However, based on the biochemical properties of DCL, that is, regulating fast structural rearrangements of the cytoskeleton and AVP biosynthesis, we propose the following hypothetical model: DCL-positive astrocytes engulf AVP-positive neurons in the shell of the SCN. Mediated by DCL, these astrocytic processes exhibit reported circadian extension/retraction (Bosler et al., 2015), thereby changing the concentration of GABA by GABA transporters such as GAT3 and secretion of astrocyte-derived glutamate (Brancaccio et al., 2017; Brancaccio et al., 2019) in the intracellular space between astrocytes and neurons. Glutamate acts on NMDA receptors in AVP neurons (Brancaccio et al., 2017). Activation of these NMDA receptors induce a Ca⁺⁺-activated signal transduction cascade activating the transcription factor cAMP response element-binding protein-3 like-1 that acts on the corresponding CRE box in the promoter of the AVP gene (Greenwood et al., 2014). Rhythmic expression in the SCN is mediated by Bmal1 and the E-box in the AVP promoter (Jin et al., 1999). Blockade of retraction/extension of astrocytic processes in DCL knockdown mice then alter the circadian fluctuation of GABA and glutamate in the synaptic cleft, thereby changing the biosynthesis of AVP. To test the validity of this hypothesis, we will focus on labeling of DCL⁺ astrocytes, for example, fluorescent constructs that are driven by the DCL promoter, and will investigate retraction/extension of astrocytic processes in both wildtype and DCL knockdown mice.

FIGURE 7 Analysis of dense core vesicles and cell/nucleus ratio by TEM of DCL knockdown and WT littermates. (a) Example of a cell classified as a neuron, characterized by a circular nucleus and a clear cytoplasmic membrane. (b) Example of a cell not classified as neuron. No clear cell boundary is visible, and the nucleus has an irregular form. The white asterisks indicating a lobed structure in the nucleus. N = nucleus, n = nucleolus, C = cytoplasm. Arrows indicate cell boundary. The scale bar represents 2 μ m. (c) Representative EM picture of a neuropeptide-positive neuron. Scale bar: 2 μ m. (d) Magnification of a putative neuropeptide-positive neuron with dense core vesicles that are further magnified in the inset showing the morphology of typical dense core vesicles that are also indicated by arrows. Scale bar: 500 nm. (e) the percentage of DCV-containing neurons at ZT8 and ZT20 in DCL knockdown mice and littermate WT controls (N = 3; p = 0.001). (f) the mean cell/nucleus ratio of putative neuropeptide-positive cells at ZT8 and ZT20 in DCL knockdown and littermate WT mice



ACKNOWLEDGMENTS

The work was supported by the Diabetes Fonds (grant 2013.81.1663 to C.P.C.). The authors thank Dr S. Michel for support in the preparation of SCN tissue for transmission electron microscopy.

DATA AVAILABILITY STATEMENT

The data that support the findings of this study are available from the corresponding author upon reasonable request.

ORCID

Erno Vreugdenhil  <https://orcid.org/0000-0002-8243-1992>

REFERENCES

- Abrahamson, E. E., & Moore, R. Y. (2001). Suprachiasmatic nucleus in the mouse: Retinal innervation, intrinsic organization and efferent projections. *Brain Research*, *916*, 172–191.
- Albus, H., Vansteensel, M. J., Michel, S., Block, G. D., & Meijer, J. H. (2005). A GABAergic mechanism is necessary for coupling dissociable ventral and dorsal regional oscillators within the circadian clock. *Current Biology*, *15*, 886–893. <https://doi.org/10.1016/j.cub.2005.03.051>
- Barca-Mayo, O., Pons-Espinal, M., Follert, P., Armirotti, A., Berdondini, L., & De Pietri Tonelli, D. (2017). Astrocyte deletion of *Bmal1* alters daily locomotor activity and cognitive functions via GABA signalling. *Nature Communications*, *8*, 14336. <https://doi.org/10.1038/ncomms14336>
- Becquet, D., Girardet, C., Guillaumond, F., François-Bellan, A.-M., & Bosler, O. (2008). Ultrastructural plasticity in the rat suprachiasmatic nucleus. Possible involvement in clock entrainment. *Glia*, *56*, 294–305. <https://doi.org/10.1002/glia.20613>
- Boekhoorn, K., Sarabdjitsingh, A., Kommerie, H., de Punder, K., Schouten, T., Lucassen, P. J., & Vreugdenhil, E. (2008). Doublecortin (DCX) and doublecortin-like (DCL) are differentially expressed in the early but not late stages of murine neocortical development. *Journal of Comparative Neurology*, *507*, 1639–1652. <https://doi.org/10.1002/cne.21646>
- Brancaccio, M., Edwards, M. D., Patton, A. P., Smyllie, N. J., Chesham, J. E., Maywood, E. S., & Hastings, M. H. (2019). Cell-autonomous clock of astrocytes drives circadian behavior in mammals. *Science*, *363*, 187–192. <https://doi.org/10.1126/science.aat4104>
- Brancaccio, M., Patton, A. P., Chesham, J. E., Maywood, E. S., & Hastings, M. H. (2017). Astrocytes control circadian timekeeping in the suprachiasmatic nucleus via glutamatergic signaling. *Neuron*, *93*, 1420–1435. <https://doi.org/10.1016/j.neuron.2017.02.030>
- Burke, J. F., Womac, A. D., Earnest, D. J., & Zoran, M. J. (2011). Mitochondrial calcium signaling mediates rhythmic extracellular ATP accumulation in suprachiasmatic nucleus astrocytes. *Journal of Neuroscience*, *31*, 8432–8440. <https://doi.org/10.1523/JNEUROSCI.6576-10.2011>
- Castel, M., Feinstein, N., Cohen, S., & Harari, N. (1990). Vasopressinergic innervation of the mouse suprachiasmatic nucleus: An immunoelectron microscopic analysis. *Journal of Comparative Neurology*, *298*, 172–187. <https://doi.org/10.1002/cne.902980204>
- Dardente, H., Menet, J. S., Challet, E., Tournier, B. B., Pévet, P., & Masson-Pévet, M. (2004). Daily and circadian expression of neuropeptides in the suprachiasmatic nuclei of nocturnal and diurnal rodents. *Brain Research. Molecular Brain Research*, *124*, 143–151. <https://doi.org/10.1016/j.molbrainres.2004.01.010>
- Deng, X.-H., Bertini, G., Palomba, M., Xu, Y.-Z., Bonaconsa, M., Nygård, M., & Bentivoglio, M. (2010). Glial transcripts and immune-challenged glia in the suprachiasmatic nucleus of young and aged mice. *Chronobiology International*, *27*, 742–767. <https://doi.org/10.3109/07420521003681498>
- Ehlen, J. C., & Paul, K. N. (2009). Regulation of light's action in the mammalian circadian clock: Role of the extrasynaptic GABAA receptor. *American journal of physiology. Regulatory, Integrative and Comparative Physiology*, *296*, R1606–R1612. <https://doi.org/10.1152/ajpregu.90878.2008>
- Faas, F. G. A., Avramut, M. C., van den Berg, B. M., Mommaas, A. M., Koster, A. J., & Ravelli, R. B. G. (2012). Virtual nanoscopy: Generation of ultra-large high resolution electron microscopy maps. *Journal of Cell Biology*, *198*, 457–469. <https://doi.org/10.1083/jcb.201201140>
- Fitzsimons, C. P., van Hooijdonk, L. W. A., Schouten, M., Zalachoras, I., Brinks, V., Zheng, T., Schouten, T. G., Saaltink, D. J., Dijkmans, T., Steindler, D. A., Verhaagen, J., Verbeek, F. J., Lucassen, P. J., de Kloet, E. R., Meijer, O. C., Karst, H., Joels, M., Oitzl, M. S., & Vreugdenhil, E. (2013). Knockdown of the glucocorticoid receptor alters functional integration of newborn neurons in the adult hippocampus and impairs fear-motivated behavior. *Molecular Psychiatry*, *18*, 993–1005. <https://doi.org/10.1038/mp.2012.123>
- Friocourt, G., Chafey, P., Billuart, P., Koulakoff, A., Vinet, M. C., Schaar, B. T., McConnell, S., Francis, F., & Chelly, J. (2001). Doublecortin interacts with mu subunits of clathrin adaptor complexes in the developing nervous system. *Molecular and Cellular Neurosciences*, *18*, 307–319. <https://doi.org/10.1006/mcne.2001.1022>
- Friocourt, G., Kappeler, C., Saillour, Y., Fauchereau, F., Rodriguez, M. S., Bahi, N., Vinet, M. C., Chafey, P., Poirier, K., Taya, S., Wood, S. A., Dargemont, C., Francis, F., & Chelly, J. (2005). Doublecortin interacts with the ubiquitin protease DFFRX, which associates with microtubules in neuronal processes. *Molecular and Cellular Neurosciences*, *28*, 153–164. <https://doi.org/10.1016/j.mcn.2004.09.005>
- Friocourt, G., Koulakoff, A., Chafey, P., Boucher, D., Fauchereau, F., Chelly, J., & Francis, F. (2003). Doublecortin functions at the extremities of growing neuronal processes. *Cerebral Cortex*, *13*, 620–626.
- Girardet, C., Lebrun, B., Cabirol-Pol, M.-J., Tardivel, C., François-Bellan, A.-M., Becquet, D., & Bosler, O. (2013). Brain-derived neurotrophic factor/TrkB signaling regulates daily astroglial plasticity in the suprachiasmatic nucleus: Electron-microscopic evidence in mouse. *Glia*, *61*, 1172–1177. <https://doi.org/10.1002/glia.22509>
- Greenwood, M., Bordieri, L., Greenwood, M. P., Rosso Melo, M., Colombari, D. S. A., Colombari, E., Paton, J. F., & Murphy, D. (2014). Transcription factor CREB3L1 regulates vasopressin gene expression in the rat hypothalamus. *Journal of Neuroscience*, *34*, 3810–3820. <https://doi.org/10.1523/JNEUROSCI.4343-13.2014>
- Hastings, M. H., Maywood, E. S., & Brancaccio, M. (2018). Generation of circadian rhythms in the suprachiasmatic nucleus. *Nature Reviews Neuroscience*, *19*, 453–469. <https://doi.org/10.1038/s41583-018-0026-z>
- Jenni, O. G., Deboer, T., & Achermann, P. (2006). Development of the 24-h rest-activity pattern in human infants. *Infant Behavior and Development*, *29*, 143–152. <https://doi.org/10.1016/j.infbeh.2005.11.001>
- Jimenez, V. A., Helms, C. M., Cornea, A., Meshul, C. K., & Grant, K. A. (2015). An ultrastructural analysis of the effects of ethanol self-administration on the hypothalamic paraventricular nucleus in rhesus macaques. *Frontiers in Cellular Neuroscience*, *9*, 260. <https://doi.org/10.3389/fncel.2015.00260>
- Jin, X., Shearman, L. P., Weaver, D. R., Zylka, M. J., de Vries, G. J., & Reppert, S. M. (1999). A molecular mechanism regulating rhythmic output from the suprachiasmatic circadian clock. *Cell*, *96*, 57–68.
- Kalsbeek, A., Fliers, E., Hofman, M. A., Swaab, D. F., & Buijs, R. M. (2010). Vasopressin and the output of the hypothalamic biological clock. *Journal of Neuroendocrinology*, *22*, 362–372. <https://doi.org/10.1111/j.1365-2826.2010.01956.x>
- Kiessling, S., Eichele, G., & Oster, H. (2010). Adrenal glucocorticoids have a key role in circadian resynchronization in a mouse model of jet lag. *Journal of Clinical Investigation*, *120*, 2600. <https://doi.org/10.1172/JCI41192>
- Kim, M. H., Cierpicki, T., Derewenda, U., Krowarsch, D., Feng, Y., Devedjiev, Y., Dauter, Z., Walsh, C. A., Otlewski, J., Bushweller, J. H., &

- Derewenda, Z. S. (2003). The DCX-domain tandems of doublecortin and doublecortin-like kinase. *Nature Structural Biology*, 10, 324–333. <https://doi.org/10.1038/nsb918>
- Koizumi, H., Tanaka, T., & Gleeson, J. G. (2006). Doublecortin-like kinase functions with doublecortin to mediate fiber tract decussation and neuronal migration. *Neuron*, 49, 55–66. <https://doi.org/10.1016/j.neuron.2005.10.040>
- Krout, K. E., Kawano, J., Mettenleiter, T. C., & Loewy, A. D. (2002). CNS inputs to the suprachiasmatic nucleus of the rat. *Neuroscience*, 10, 73–92.
- Lee, H. S., Nelsm, J. L., Nguyen, M., Silver, R., & Lehman, M. N. (2003). The eye is necessary for a circadian rhythm in the suprachiasmatic nucleus. *Nature Neuroscience*, 6, 111–112. <https://doi.org/10.1038/nn1006>
- Leone, M. J., Beaulieu, C., Marpegan, L., Simon, T., Herzog, E. D., & Golombek, D. A. (2015). Glial and light-dependent glutamate metabolism in the suprachiasmatic nuclei. *Chronobiology International*, 32, 573–578. <https://doi.org/10.3109/07420528.2015.1006328>
- Li, J.-D., Burton, K. J., Zhang, C., Hu, S.-B., & Zhou, Q.-Y. (2009). Vasopressin receptor V1a regulates circadian rhythms of locomotor activity and expression of clock-controlled genes in the suprachiasmatic nuclei. *American Journal of Physiology, Regulatory, Integrative and Comparative Physiology*, 296, R824–R830. <https://doi.org/10.1152/ajpregu.90463.2008>
- Lipka, J., Kapitein, L. C., Jaworski, J., & Hoogenraad, C. C. (2016). Microtubule-binding protein doublecortin-like kinase 1 (DCLK1) guides kinesin-3-mediated cargo transport to dendrites. *EMBO Journal*, 35, 302–318. <https://doi.org/10.15252/embj.201592929>
- Liu, J. S., Schubert, C. R., Fu, X., Fourniol, F. J., Jaiswal, J. K., Houdusse, A., Stultz, C. M., Moores, C. A., & Walsh, C. A. (2012). Molecular basis for specific regulation of neuronal kinesin-3 motors by doublecortin family proteins. *Molecular Cell*, 47, 707–721. <https://doi.org/10.1016/j.molcel.2012.06.025>
- Marpegan, L., Swannstrom, A. E., Chung, K., Simon, T., Haydon, P. G., Khan, S. K., Liu, A. C., Herzog, E. D., & Beaulieu, C. (2011). Circadian regulation of ATP release in astrocytes. *Journal of Neuroscience*, 31, 8342–8350. <https://doi.org/10.1523/JNEUROSCI.6537-10.2011>
- Meijer, J. H., Colwell, C. S., Rohling, J. H. T., Houben, T., & Michel, S. (2012). Dynamic neuronal network organization of the circadian clock and possible deterioration in disease. In A. Kalsbeek, M. Meroz, T. Roenneberg, & R. G. Foster (eds.), *The neurobiology of circadian timing* (Vol. 199, 1st ed., pp. 143–162). Elsevier B.V. <https://doi.org/10.1016/B978-0-444-59427-3.00009-5>
- Mieda, M. (2019). The network mechanism of the central circadian pacemaker of the SCN: Do AVP neurons play a more critical role than expected? *Frontiers in Neuroscience*, 13, 139. <https://doi.org/10.3389/fnins.2019.00139>
- Mieda, M., Ono, D., Hasegawa, E., Okamoto, H., Honma, K.-I., Honma, S., & Sakurai, T. (2015). Cellular clocks in AVP neurons of the SCN are critical for Interneuronal coupling regulating circadian behavior rhythm. *Neuron*, 85, 1103–1116. <https://doi.org/10.1016/j.neuron.2015.02.005>
- Moldavan, M., Cravetchi, O., Williams, M., Irwin, R. P., Aicher, S. A., & Allen, C. N. (2015). Localization and expression of GABA transporters in the suprachiasmatic nucleus. *European Journal of Neuroscience*, 42, 3018–3032. <https://doi.org/10.1111/ejn.13083>
- Moore, R. Y., Speh, J. C., & Leak, R. K. (2002). Suprachiasmatic nucleus organization. *Cell and Tissue Research*, 309, 89–98. <https://doi.org/10.1007/s00441-002-0575-2>
- Moores, C. A., Perderiset, M., Francis, F., Chelly, J., Houdusse, A., & Milligan, R. A. (2004). Mechanism of microtubule stabilization by doublecortin. *Molecular Cell*, 14, 833–839. <https://doi.org/10.1016/j.molcel.2004.06.009>
- Morin, L. P. (2013). Neuroanatomy of the extended circadian rhythm system. *Experimental Neurology*, 243, 4–20. <https://doi.org/10.1016/j.expneurol.2012.06.026>
- Ng, F. S., Tangredi, M. M., & Jackson, F. R. (2011). Glial cells physiologically modulate clock neurons and circadian behavior in a calcium-dependent manner. *Current Biology*, 21, 625–634. <https://doi.org/10.1016/j.cub.2011.03.027>
- Panagiotou, M., & Deboer, T. (2020). Effects of chronic dim-light-at-night exposure on sleep in young and aged mice. *Neuroscience*, 426, 154–167. <https://doi.org/10.1016/j.neuroscience.2019.11.033>
- Park, J., Zhu, H., O'Sullivan, S., Ogunnaike, B. A., Weaver, D. R., Schwaber, J. S., & Vadigepalli, R. (2016). Single-cell transcriptional analysis reveals novel neuronal phenotypes and interaction networks involved in the central circadian clock. *Frontiers in Neuroscience*, 10, 481. <https://doi.org/10.3389/fnins.2016.00481>
- Prolo, L. M., Takahashi, J. S., & Herzog, E. D. (2005). Circadian rhythm generation and entrainment in astrocytes. *Journal of Neuroscience*, 25, 404–408. <https://doi.org/10.1523/JNEUROSCI.4133-04.2005>
- Saaltink, D.-J., Håvik, B., Verissimo, C. S., Lucassen, P. J., & Vreugdenhil, E. (2012). Doublecortin and doublecortin-like are expressed in overlapping and non-overlapping neuronal cell population: Implications for neurogenesis. *Journal of Comparative Neurology*, 520, 2805–2823. <https://doi.org/10.1002/cne.23144>
- Saaltink, D.-J., van Zwet, E. W., & Vreugdenhil, E. (2020). Doublecortin-like is implicated in adult hippocampal neurogenesis and in motivational aspects to escape from an aversive environment in male mice. *eNeuro*, 7, 1–12. <https://doi.org/10.1523/ENEURO.0324-19.2020>
- Schaar, B. T., Kinoshita, K., & McConnell, S. K. (2004). Doublecortin microtubule affinity is regulated by a balance of kinase and phosphatase activity at the leading edge of migrating neurons. *Neuron*, 41, 203–213.
- Seibler, J., Kleinridders, A., Küter-Luks, B., Niehaves, S., Brüning, J. C., & Schwenk, F. (2007). Reversible gene knockdown in mice using a tight, inducible shRNA expression system. *Nucleic Acids Research*, 35, e54. <https://doi.org/10.1093/nar/gkm122>
- Shin, E., Kashiwagi, Y., Kuriu, T., Iwasaki, H., Tanaka, T., Koizumi, H., Gleeson, J. G., & Okabe, S. (2013). Doublecortin-like kinase enhances dendritic remodeling and negatively regulates synapse maturation. *Nature Communications*, 4, 1440–1414. <https://doi.org/10.1038/ncomms2443>
- Sonneville, R., Guidoux, C., Barrett, L., Viltart, O., Mattot, V., Polito, A., Siami, S., de la Grandmaison, G. L., Blanchard, A., Singer, M., Annane, D., Gray, F., Brouland, J. P., & Sharshar, T. (2010). Vasopressin synthesis by the magnocellular neurons is different in the supraoptic nucleus and in the paraventricular nucleus in human and experimental septic shock. *Brain Pathology*, 20, 613–622. <https://doi.org/10.1111/j.1750-3639.2009.00355.x>
- Stenvers, D. J., van Dorp, R., Foppen, E., Mendoza, J., Opperhuizen, A.-L., Fliers, E., Bisschop, P. H., Meijer, J. H., Kalsbeek, A., & Deboer, T. (2016). Dim light at night disturbs the daily sleep-wake cycle in the rat. *Scientific Reports*, 6, 1–12. <https://doi.org/10.1038/srep35662>
- Bosler, O., Girardet, C., Franc, J.-L., Becquet, D., & Francois-Bellan, A.-M. (2015). Structural plasticity of the circadian timing system. *An overview from flies to mammals*, 38, 50–64. <https://doi.org/10.1016/j.yfme.2015.02.001>
- Tso, C. F., Simon, T., Greenlaw, A. C., Puri, T., Mieda, M., & Herzog, E. D. (2017). Astrocytes regulate daily rhythms in the suprachiasmatic nucleus and behavior. *Current Biology*, 27, 1–8. <https://doi.org/10.1016/j.cub.2017.02.037>
- Vreugdenhil, E., Kolk, S. M., Boekhoorn, K., Fitzsimons, C. P., Schaaf, M., Schouten, T., Sarabdjitsingh, A., Sibug, R., & Lucassen, P. J. (2007). Doublecortin-like, a microtubule-associated protein expressed in radial glia, is crucial for neuronal precursor division and radial process stability. *European Journal of Neuroscience*, 25, 635–648. <https://doi.org/10.1111/j.1460-9568.2007.05318.x>
- Walz, W., & Lang, M. K. (1998). Immunocytochemical evidence for a distinct GFAP-negative subpopulation of astrocytes in the adult rat hippocampus. *Neuroscience Letters*, 257, 127–130. [https://doi.org/10.1016/s0304-3940\(98\)00813-1](https://doi.org/10.1016/s0304-3940(98)00813-1)
- Wen, S., Ma, D., Zhao, M., Xie, L., Wu, Q., Gou, L., Zhu, C., Fan, Y., Wang, H., & Yan, J. (2020). Spatiotemporal single-cell analysis of gene expression in the mouse suprachiasmatic nucleus. *Nature Neuroscience*, 23, 456–467. <https://doi.org/10.1038/s41593-020-0586-x>



- Yamaguchi, Y., Suzuki, T., Mizoro, Y., Kori, H., Okada, K., Chen, Y., Fustin, J. M., Yamazaki, F., Mizuguchi, N., Zhang, J., Dong, X., Tsujimoto, G., Okuno, Y., Doi, M., & Okamura, H. (2013). Mice genetically deficient in vasopressin V1a and V1b receptors are resistant to jet lag. *Science*, 342, 85–90. <https://doi.org/10.1126/science.1238599>
- Yoshikawa, T., Nakajima, Y., Yamada, Y., Enoki, R., Watanabe, K., Yamazaki, M., Sakimura, K., Honma, S., & Honma, K. (2015). Spatio-temporal profiles of arginine vasopressin transcription in cultured suprachiasmatic nucleus. *European Journal of Neuroscience*, 42, 2678–2689. <https://doi.org/10.1111/ejn.13061>

How to cite this article: Coomans, C., Saaltink, D.-J., Deboer, T., Tersteeg, M., Lanooij, S., Schneider, A. F., Mulder, A., van Minnen, J., Jost, C., Koster, A. J., & Vreugdenhil, E. (2021). Doublecortin-like expressing astrocytes of the suprachiasmatic nucleus are implicated in the biosynthesis of vasopressin and influences circadian rhythms. *Glia*, 69(11), 2752–2766. <https://doi.org/10.1002/glia.24069>